
Adaptive Temperature Scaling with Conformal Prediction

Nikita Kotelevskii

Department of ML, MBZUAI, UAE
 nikita.kotelevskii@mbzuai.ac.ae

Mohsen Guizani

Department of ML, MBZUAI, UAE

Eric Moulines

CMAP, École polytechnique, France
 Department of ML, MBZUAI, UAE

Maxim Panov

Department of ML, MBZUAI, UAE
 maxim.panov@mbzuai.ac.ae

Abstract

Conformal prediction enables the construction of high-coverage prediction sets for any pre-trained model, guaranteeing that the true label lies within the set with a specified probability. However, these sets do not provide probability estimates for individual labels, limiting their practical use. In this paper, we propose, to the best of our knowledge, the first method for assigning calibrated probabilities to elements of a conformal prediction set. Our approach frames this as an adaptive calibration problem, selecting an input-specific temperature parameter to match the desired coverage level. Experiments on several challenging image classification datasets demonstrate that our method maintains coverage guarantees while significantly reducing expected calibration error.

1 Introduction

In modern applications – often in high-stakes domains – classification models, particularly deep neural networks, are used ubiquitously. In this context, quantifying predictive uncertainty accurately is of decisive importance as it allows one to abstain from non-confident predictions or just informs the user on the likelihood of prediction error [12, 6, 7].

Among others, two important uncertainty quantification problems are considered in machine learning literature:

- *Calibration* methods adjust the model’s output probabilities to reflect better an expected accuracy for each input [9, 28].
- *Conformal prediction* generates prediction sets guaranteed to contain the true label with a specified probability [1, 24].

While these approaches aim to quantify predictive uncertainty, each offers a different perspective and comes with its own limitations. In particular, calibration techniques focus only on the overall error probability (confidence), ignoring the probability distribution across classes. Conformal prediction only produces sets of labels and does not assign probabilities within those sets.

In this work, we aim to combine probability calibration with confidence-set construction. Ideally, we want the best of both worlds: a small prediction set with coverage guarantees plus a well-defined probability distribution over the labels in the set. We take a first step toward bridging calibration and conformal prediction by introducing a family of methods that supply each conformal prediction set with calibrated probabilities for its labels.

Category	Method	α -agnostic	Adaptive quantile	Bypass cal. data	Key idea
α -specific	<i>ATS-CP-GQ</i> : Global Quantile	\times	\times	\times	Global thresholding : compute a single $(1 - \alpha)$ -quantile q_α from all calibration scores, form $C_\alpha(x) = \{y: V(x, y) \leq q_\alpha\}$, then search $\tau_\alpha(x)$ so that $\sum_{y \in C_\alpha(x)} \hat{p}(y x, \tau_\alpha) = 1 - \alpha$.
	<i>ATS-CP-AQ</i> : Adaptive Quantile	\times	\checkmark	\checkmark	Learned threshold : train quantile regressor $QR_\alpha(x)$ on D_{cal}^V to predict $q_\alpha(x)$ per input; use $C_\alpha(x) = \{y: V(x, y) \leq q_\alpha(x)\}$, then binary-search $\tau_\alpha(x)$ for coverage.
α -agnostic	<i>ATS-CP-MGQ</i> : Multi-Global Quantile	\checkmark	\checkmark	\times	Class-wise calibration : for each label y , estimate $\alpha_y = 1 - \hat{F}(V(y, x_j))$, find τ_y^* so that $\sum_{k \in C_{\alpha_y}(x)} \hat{p}(k x, \tau_y^*) = 1 - \alpha_y$, then aggregate the K distributions.
	<i>ATS-CP-MAQ</i> : Multi-Adaptive Quantile	\checkmark	\checkmark	\checkmark	Instance-specific thresholds : train Multi-Head Quantile regression (on a set of predefined α -s or a Conditional Normalizing flow [4] on D_{cal}^V), then predict multiple quantiles, build each $C_{\alpha_j}(x)$, calibrate $\tau_j^*(x)$ for each, and merge resulting distributions.

Table 1: Categorization of the proposed probability calibration approaches. ‘‘Bypass cal. data’’ means whether the approach explicitly uses scores from the calibration dataset *during inference* or utilizes some amortized models for each x .

The main **contributions** of this work are as follows.

1. We formalize *probability assignment* within conformal prediction by defining a principled mapping from conformity scores to label probabilities within the prediction set, thus producing a fully calibrated distribution over the set.
2. We introduce the *Adaptive Temperature Scaling with Conformal Prediction (ATS-CP)* framework, which computes an input-specific temperature scaling factor $\tau_\alpha := \tau_\alpha(x)$ such that the adjusted probabilities of the conformal set sum to the target coverage level $1 - \alpha$. Our ATS-CP framework is a fully post-hoc, distribution-free approach – no retraining of the base model is needed, and it makes minimal assumptions.
3. We present a family of ATS-CP extensions including instance-adaptive quantile methods and α -agnostic variants that eliminate the need to choose a specific miscoverage level α upfront.
4. We provide extensive experiments showing that ATS-CP variants (by construction) preserve the required coverage across datasets while substantially reducing calibration error compared to the uncalibrated base model and existing methods.

2 Background

We consider a standard K -class classification problem. Let

$$\{(x_i, y_i)\}_{i=1}^{(n+m)} \subset \mathcal{X} \times \mathcal{Y}, \quad \mathcal{Y} = \{1, \dots, K\}$$

be a dataset of $n + m$ i.i.d. pairs drawn from an unknown distribution $p(x, y)$. We split this data into a *training set* D_{tr} of m points to learn a base model and a *calibration set* D_{cal} of n points, that is used for conformal prediction process. A base predictor $p_\theta(y | x)$ with parameters θ (e.g., the weights of a deep neural network) is trained on the training set by minimizing a suitable loss (e.g., cross-entropy). At test time, p_θ produces a probability vector $(p_\theta(y = 1 | x), \dots, p_\theta(y = K | x))$ for a new input object x .

Confidence calibration. Despite the impressive discriminative performance, modern deep neural networks often exhibit *miscalibration*, meaning the predicted probabilities do not align with the actual frequency of correct predictions [9]. A model is considered confidence-calibrated if, for all confidences $p \in [0, 1]$, the model is correct p proportion of the time:

$$\Pr(Y_* = \arg \max_y p_\theta(y | X_*) \mid \max_y p_\theta(y | X_*) = p) = p,$$

where the probability is over the joint distribution of X_* and Y_* . Heuristic approaches like temperature scaling [9], isotonic regression [28] or Platt scaling [22] can improve calibration on average, but do not offer any formal calibration guarantees.

Conformal Prediction (CP). Conformal Prediction [24, 1] provides distribution-free, model-agnostic coverage guarantees by producing, for each new input x , a *prediction set* $C_\alpha(x) \subseteq \mathcal{Y}$, such that

$$\Pr(Y_* \in C_\alpha(X_*)) \geq 1 - \alpha,$$

under the only assumption that calibration data D_{cal} and test point (X_*, Y_*) are exchangeable. In the definition above, $\alpha \in (0, 1)$ is a user-specified miscoverage rate. Typically, α is chosen to be small, therefore predicted conformal set $C_\alpha(x)$ contains the ground truth label y_* with high probability of at least $1 - \alpha$. Generally, for conformal prediction, two types of coverage are desirable:

- *Marginal coverage* [1]: $\Pr(Y_* \in C_\alpha(X_*)) \geq 1 - \alpha$ on average over the joint distribution of X_* , Y_* and D_{cal} .
- *Conditional coverage* [20, 4]: $\Pr(Y_* \in C_\alpha(X_*) \mid X_* = x_*) \geq 1 - \alpha$ for each x_* . Exact conditional coverage is impossible with finite data [5], but approximate methods aim to improve consistency across inputs.

To use the conformal prediction, one needs to choose a score function:

$$V: \mathcal{X} \times \mathcal{Y} \rightarrow \mathbb{R},$$

where larger amplitudes of $V(x, y)$ indicates a less plausible label y for input x . Common simple choice in classification is $V_{prob}(x, y) = 1 - p_\theta(y \mid x)$.

Given a calibration set $\{(x_j, y_j)\}_{j=1}^n$, we compute the scores $\{V(x_j, y_j)\}_{j=1}^n$ and form the empirical CDF:

$$\hat{F}_V(t) = \frac{1}{n} \sum_{j=1}^n \mathbf{1}\{V(x_j, y_j) \leq t\}.$$

In classical conformal prediction, for the miscoverage rate α chosen in advance, we compute q_α , the $\lceil (1 - \alpha)(n + 1) \rceil / n$ -quantile of the empirical score distribution \hat{F}_V . Then for any test point x , the *conformal prediction set* is

$$C_\alpha(x) = \{y: V(x, y) \leq q_\alpha\}.$$

By construction, for the ground truth Y_* the inequality holds $\Pr(Y_* \in C_\alpha(X_*)) \geq 1 - \alpha$ marginally.

One of the limitations of CP is that it can provide only the set of possible labels $C_\alpha(x)$ without assigning any probabilities to its elements. In many applications (e.g., decision-making under uncertainty, classification with abstention), one requires a full probability distribution that is both calibrated and respects the conformal coverage. This limitation motivates our Adaptive Temperature Scaling approach, which provides label-wise probabilities while preserving conformal coverage.

3 Adaptive Temperature Scaling with Conformal Prediction

We aim to *induce* a calibrated probability distribution $\tilde{p}_\theta(y \mid x, \tau_\alpha)$ for any test point x , that (i) retains the coverage guarantee on the conformal set and (ii) preserves the same ranking of the labels as the score function V . Our approach proceeds in two steps: for a new input x , we (1) construct a conformal prediction set at a chosen miscoverage level α (not necessarily fixed); (2) convert the scores in this set into a probability distribution and adjust an input-specific temperature $\tau > 0$. Under mild assumptions (see Lemma A.1), for each α , there is a unique *optimal temperature* τ_α , which can be efficiently found via binary search.

Tempered probabilities. Given the conformal set $C_\alpha(x)$, we convert the score values for all labels into a probability distribution via a temperature-scaled softmax function:

$$\tilde{p}_V(y \mid x, \tau) = \frac{\exp(-\log V(x, y)/\tau)}{\sum_{y'} \exp(-\log V(x, y')/\tau)}, \quad (1)$$

Algorithm 1: ATS-CP

Input: Base model p_θ ; calibration set $D_{cal} = \{(x_j, y_j)\}_{j=1}^n$; miscoverage α ; score V ; tolerance ε ; max iters M .
Output: Calibrated probability vector \tilde{p} .

// **Offline**

- 1 Compute $D_{cal}^V = \{(x_j, V(x_j, y_j))\}_{j=1}^n$;
 // Then either
- 2 $q_\alpha \leftarrow \text{Quantile}_{1-\alpha}(\{V(x_j, y_j)\})$;
 // or
- 3 fit QR on D_{cal}^V to predict (possibly many)
 $q_\alpha(x)$;
- // **Online (per test x_*)**
- 4 Compute $\{V(x_*, y)\}_{y=1}^K$;
- 5 **for each α do**
 Form $C_\alpha(x_*) = \{y: V(x_*, y) \leq q_\alpha\}$;
 Select
 $\tau_\alpha \leftarrow \text{SelectTau}(C_\alpha(x_*),$
 $\{-\log V(x_*, y)\}_{y=1}^K, 1 - \alpha, \varepsilon, M)$
- 8 Aggregate $\{\tilde{p}_\alpha(y | x_*, \tau_\alpha)\}_\alpha$ into
 $\tilde{p}(y | x_*)$
- 9 **return** $\tilde{p}(y | x_*)$

Algorithm 2: SelectTau

Input: Conf. set $C_\alpha(x_*)$; logits $\{s_y\}_{y=1}^K$;
target mass $1 - \alpha$; tolerance ε ; max iters M .
Output: Temperature τ_α satisfying
$$\sum_{y \in C_\alpha(x_*)} \text{softmax}(s_y / \tau_\alpha) = 1 - \alpha.$$

1 Initialize
 $\tau_{\min} = 10^{-6}, \tau_{\max} = 10^6, \tau = 1$. **for**
 $t = 1, \dots, M$ **do**

2 Compute
 $S = \sum_{y \in C_\alpha(x_*)} \text{softmax}(s_y / \tau)$.

3 **if** $|S - (1 - \alpha)| < \varepsilon$ **then**
4 **return** τ

5 **else**
6 **if** $S > (1 - \alpha)$ **then**
7 $\tau_{\min} = \tau$

8 **else**
9 $\tau_{\max} = \tau$

10 Update
 $\tau = \frac{\tau_{\min} + \tau_{\max}}{2}$.

11 **return** τ

Figure 1: **ATS-CP and SelectTau Subroutine.** The two-phase ATS-CP algorithm is shown on the left. In the *Offline* stage, we use a pre-trained model to compute calibration scores and either select a global quantile q_α or train a quantile regressor that produces $q_\alpha(x)$ for a given x . In the *Online* stage, for each test point x_* (and possibly for each α) we form the conformal set $C_\alpha(x_*)$, call the SELECTTAU routine to find the per-instance temperature τ_α , and output the calibrated probability vector $\tilde{p}(y | x_*)$ (optionally aggregating results across multiple α). On the right, the SELECTTAU subroutine is shown: it performs a bisection search on τ and returns the final τ .

where $\tau > 0$ is a *temperature* parameter. Smaller τ yields a sharper distribution concentrated on low-score labels, while larger τ spreads mass more uniformly. We choose the value τ_α that gives exact conformal coverage:

$$\sum_{y \in C_\alpha(x)} \tilde{p}_V(y | x, \tau_\alpha) = 1 - \alpha. \quad (2)$$

Since conformal sets vary for different inputs x , this procedure of seeking τ_α results in *input-dependent (adaptive) calibration*. As the left-hand side of equation (2) is continuous and strictly decreasing in τ_α , one can solve (2) efficiently by binary search over $\tau_\alpha \in [\tau_{\min}, \tau_{\max}]$.

We refer to our proposed conformal calibration procedure as *Adaptive Temperature Scaling with Conformal Prediction (ATS-CP)*. Algorithm 1 presents the overall ATS-CP procedure, which consists of two stages (offline and online). We compute nonconformity scores on the calibration set in the *offline phase*. Then we either (a) select a global quantile q_α , or (b) train a quantile regression (QR) model to predict an input-dependent $q_\alpha(x)$ for each x ; see Section 3.1 and Appendix G for details. For multiple miscoverage levels, we train a multi-head QR (or a conditional normalizing flow [4]) and aggregate its outputs into one calibrated probability distribution; see Section 3.2 and Appendix G.

In the *online phase*, for each test point x we (i) form the conformal set $C_\alpha(x)$ (for each required α level);, (ii) run the SELECTTAU subroutine (Algorithm 2) to find the instance-specific temperature $\tau_\alpha(x)$; (iii) compute the calibrated output distribution $\tilde{p}_V(\cdot | x, \tau_\alpha)$. This per-instance tempering preserves the conformal coverage guarantee for each input x (see Lemma A.1).

Equivalence transforms. Any monotonic transformation $\phi: \mathbb{R} \rightarrow \mathbb{R}$ of the scores leaves the conformal set unchanged (since it preserves the score ordering). For example, if we take the score $V_{prob}(x, y)$ and define $\phi(V) = \frac{1}{1 - V}$, then $\tilde{p}_{\phi \circ V}(y | x, \tau_\alpha) = \text{Softmax}(-\log \phi(V(x, y)) / \tau_\alpha) = \text{Softmax}(\log p_\theta(y | x) / \tau_\alpha)$, which recovers the standard temperature scaling on the base model's logits [18]. We include this scenario (scaling the base model's probabilities) in our experiments.

3.1 Calibration Methods

We detail the proposed framework in Appendix G. In this section and Table 1, we briefly describe the main idea behind it.

The approach described in the previous section depends critically on choosing a miscoverage level α .¹ However, conformal prediction literature rarely offers concrete guidance on picking α even for building sets, not saying for calibration purposes. In practice, practitioners choose small values of α ($\alpha = 0.1$ or $\alpha = 0.2$ are standard choices in many papers [1, 20, 21]). Different values of α lead to different quantile thresholds q_α and, thus, to different τ_α and calibrated vectors $\tilde{p}(y | x, \tau_\alpha)$; see equation (2).

We emphasize that *the choice of α is not a primary concern of our paper* but rather an open problem for the area of conformal prediction. As a first step towards resolving this difficulty, we extend our approach with a family of calibration methods that bypass selecting a specific value for α , allowing a user to specify a set (or even without specification).

Therefore, we organize calibration methods into two families:

- **α -specific methods**, which fix a single global miscoverage rate α once for all test points. One can further either use the corresponding quantile q_α from the calibration dataset or predict it for each of the covariates, i.e., $q_\alpha(x)$.
- **α -agnostic methods**, which adaptively determine α (and hence q_α) on a per-input basis. This idea leads to two approaches: one leverages calibration set D_{cal}^V and uses the empirical distribution of scores, while the other chooses α -s adaptively.

Therefore, we introduce a family of *Adaptive Temperature Scaling with Conformal Prediction (ATS-CP)* methods. We have four different variations: Global Quantile (GQ), Adaptive Quantile (AQ), Multiple Global Quantiles (MGQ), and finally Multiple Adaptive Quantiles (MAQ). Table 1 summarizes them. Each method then uses the adaptive-tempering subroutine (Algorithm 2) to turn scores into a probability vector $\tilde{p}(y | x, \tau_\alpha)$ satisfying the corresponding coverage constraint, and then aggregate them (if needed) to a single vector $\tilde{p}(y | x)$.

3.2 Aggregation of Calibrated Distributions

As shown in Table 1, the α -agnostic methods produce multiple calibrated probability vectors. In practice, however, we require a single calibrated categorical output. This raises the question: How can we aggregate several calibrated distributions into one?

To address this, we frame aggregation as the problem of minimizing an expected Bregman divergence [3, 8]. The Kullback–Leibler (KL) divergence is the natural choice for categorical distributions.

Given calibrated vectors $\{\tilde{p}_j\}_{j=1}^m$ (each corresponding to a different miscoverage level α_j and, therefore, different τ_{α_j}), one can form two types of KL-based centroids:

- **Forward-KL centroid (arithmetic mean):**

$$p_{\text{avg}} = \arg \min_c \mathbb{E}_{\tilde{p}} D_{\text{KL}}(\tilde{p} \| c) \approx \frac{1}{m} \sum_{j=1}^m \tilde{p}_j.$$

- **Reverse-KL centroid (geometric mean):**

$$p_{\text{central}} = \arg \min_c \mathbb{E}_{\tilde{p}} D_{\text{KL}}(c \| \tilde{p}) \approx \text{Softmax}\left(\frac{1}{m} \sum_{j=1}^m \log \tilde{p}_j\right).$$

These closed-form solutions yield a representative “central” vector. Other options are discussed in Appendix B.

¹In practice, α controls how much probability mass is forced onto the conformal set, and hence directly affects the resulting temperature τ_α and the shape of the calibrated distribution.

4 Related Work

Deep neural networks are often miscalibrated — their predicted confidence levels can diverge from actual accuracy — and many techniques have been proposed to address this. While certain training-time strategies (e.g., label smoothing [19]) can improve calibration, here we focus on post-hoc calibration methods, as these better align with conformal prediction’s black-box setting.

Classical post-hoc methods – Temperature Scaling [9], Platt Scaling [22], and Isotonic Regression [28] – remain popular due to their low computational cost and ease of implementation. Multiple extensions have been proposed to increase the flexibility of these calibration methods. For example, Dirichlet Calibration [16] extends Temperature Scaling with a more expressive parametric mapping. However, all such techniques share a fundamental limitation: each approach fits a single global transform to improve *marginal* calibration across a validation set and does not adapt to individual inputs. This means even a correct high-confidence prediction gets overly smoothed, becoming less confident than necessary. Consequently, these global methods cannot guarantee that a prediction’s confidence truly reflects the uncertainty for a specific example.

To address this limitation, researchers have proposed *adaptive* calibration methods. Notably, some works [26, 13, 2] introduce Adaptive Temperature Scaling (ATS), which learns an input-dependent temperature function $T(x)$ that provides a different temperature for each example. The core idea is to train a dedicated model (e.g., a small neural network) that outputs an appropriate temperature value given an input x . While these methods introduce richer, input- or class-conditional transforms, they remain largely heuristic: they often lack distribution-free coverage guarantees and can overfit on small calibration sets.

Meanwhile, conformal prediction [1, 24] offers *provable* control of miscoverage by outputting prediction *sets* rather than scalar confidences. However, classical conformal methods do not directly yield calibrated probability vectors, and naive extensions can sacrifice sharpness or incur prohibitive costs in multiclass settings.

Unlike prior ATS methods, which require additional training and do not provide formal coverage guarantees, our ATS-CP approach is a post-hoc method that yields instance-specific calibrated probabilities with distribution-free coverage assurances.

Some recent works have targeted the relation between conformal prediction and calibration, noting that calibration can sometimes lead to unnecessary large conformal prediction sets [27]. It was shown [27] that specially adapted calibration methods may help improve conformal prediction efficiency. From a different perspective, the work [11] aims to minimize the dependence of conformal prediction values on the output probability values altogether.

Our contribution. We propose an adaptive (to each input object x) *conformal-tempering* framework that (i) retains conformal coverage guarantees, (ii) yields sharp, instance-wise probability vectors via a single temperature parameter, and (iii) scales efficiently to multiclass problems.

5 Experiments

In this section, we evaluate proposed calibration methods in a series of experiments. Our experiments consider a controlled toy example with available ground-truth conditional distribution $p(y | x)$ as well as classical image classification datasets. Additionally, we consider an ablation study on the choice of α .

For all these experiments, we apply the same probability *contamination procedure* to better highlight each method’s improvements. This yields intentionally miscalibrated prediction probabilities from the base model while preserving its original accuracy. In the next section, we describe this procedure in detail.

5.1 Probability Contamination Noise Model

Standard image-classification datasets (e.g., CIFAR-10, CIFAR-100) contain almost zero aleatoric uncertainty [14], so the true conditional distribution $p(y | x)$ is close to the Dirac delta function. Consequently, even overconfident neural networks can appear well-calibrated. To create a more

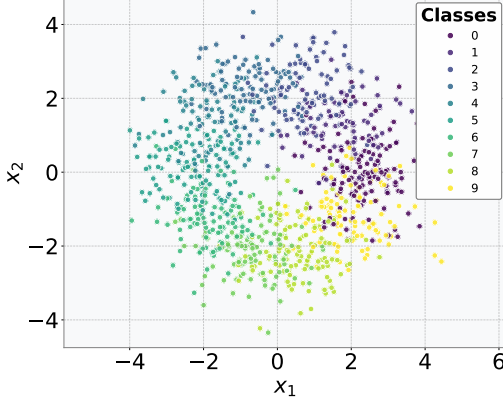


Figure 2: Synthetic data for our toy experiment: a mixture of $K = 10$ 2D isotropic Gaussians whose centers are uniformly spaced around a circle of radius 2.25.

Method	Mean \pm Std
Our Methods	
ATS-CP-GQ (prob, $\alpha = 0.15$)	0.1074 ± 0.0023
ATS-CP-GQ (score, $\alpha = 0.15$)	0.0945 ± 0.0011
ATS-CP-AQ (prob, $\alpha = 0.2$)	0.1045 ± 0.0053
ATS-CP-AQ (score, $\alpha = 0.2$)	0.1062 ± 0.0063
ATS-CP-MAQ (scores, CondNF)	0.1829 ± 0.0172
ATS-CP-MAQ (probs, MultiQR)	0.0777 ± 0.0050
Competitors	
Base Model	0.1641 ± 0.0021
Platt Scaling	0.1613 ± 0.0122
Isotonic Regression	0.1319 ± 0.0137
Dirichlet Scaling	0.1741 ± 0.0215
Temperature Scaling	0.1698 ± 0.0013
ATSC	0.4569 ± 0.3017

Table 2: Calibration error (CPSME) on the synthetic dataset, averaged across $\alpha \in \{0.05, \dots, 0.50\}$ and five random seeds. Lower values indicate better calibration. Mean \pm std is shown for the method. The best result is shown in **bold**, and the second best is underlined. Our methods (top) achieve substantially lower error than all baselines (bottom)

challenging test for calibration, we intentionally degrade the model’s confidence calibration by “contaminating” its predicted probability vectors with random temperature scaling.

Specifically, we partition the K classes evenly into three groups, which we label $\{\mathcal{G}_{\text{under}}, \mathcal{G}_{\text{normal}}, \mathcal{G}_{\text{over}}\}$, and for each test example (x, y) draw a temperature at random:

$$T = \begin{cases} \text{Uniform}\{2.0, 3.0, 5.0\}, & y \in \mathcal{G}_{\text{under}}, \\ 1.0, & y \in \mathcal{G}_{\text{normal}}, \\ \text{Uniform}\{0.25, 0.5, 0.75\}, & y \in \mathcal{G}_{\text{over}}. \end{cases}$$

We then apply temperature scaling to the original prediction $p_\theta(y | x)$:

$$\tilde{p}_\theta(y | x) := \text{Softmax}\left[\frac{1}{T} \log p_\theta(y | x)\right].$$

By construction, $T < 1$ sharpens the distribution (leading to overconfidence), $T = 1$ leaves it unchanged, and $T > 1$ smooths it (leading to underconfidence). These resulting “noisy” probability vectors serve as the base model’s outputs for all subsequent experiments. Importantly, this contamination procedure does not affect the model’s accuracy; it only degrades the calibration of its predictions.

5.2 Synthetic Data Experiment

We conduct a controlled synthetic experiment to quantify how well the calibrated probabilities align with the true distribution. Our synthetic dataset consists of $K = 10$ isotropic Gaussian clusters evenly spaced on a circle (see Figure 2). Because we know the true Gaussian mixture distribution, we can compute the exact conditional label density $p(y | x)$; see Appendix F for details. We chose the Gaussians to overlap slightly, ensuring the classification task isn’t trivial and that meaningful calibration errors remain.

For each test point x_* , we construct the ground-truth conformal set $C_\alpha^*(x_*)$ at level α by sorting classes in descending order of probabilities in $p(y | x_*)$ and including classes until their cumulative sum first exceeds $1 - \alpha$ (cf. equation (2)).

To simulate miscalibration, we draw n samples $\{x_i\}_{i=1}^n$ from the GMM, compute their true probabilities $p(y | x_i)$, and then apply the contamination procedure described in Section 5.1 to obtain perturbed probabilities $\tilde{p}(y | x_i)$. These perturbed probabilities $\tilde{p}(y | x_i)$ will be considered as the outputs of our predictive model and are the ones we will calibrate.

Dataset	AQ (p)	AQ (s)	GQ (p)	GQ (s)	MAQ (p, CondNF)	ATSC	Dirichlet	Iso. Reg.	Platt	Temp. Scl.	Base
CIFAR-10	3.11 ± 0.65	2.98 ± 0.47	2.02 ± 0.46	2.04 ± 0.46	1.96 ± 0.36	1.68 ± 1.03	4.25 ± 0.55	0.94 ± 0.36	6.04 ± 0.38	11.16 ± 0.62	13.01 ± 0.21
CIFAR-100	5.50 ± 1.87	6.30 ± 1.76	3.74 ± 0.16	7.06 ± 0.82	18.84 ± 3.21	31.46 ± 20.67	18.30 ± 0.42	9.93 ± 1.11	20.98 ± 0.36	29.07 ± 0.60	28.58 ± 0.48
TinyImageNet	5.17 ± 1.83	6.77 ± 0.88	4.72 ± 0.46	7.26 ± 0.89	15.27 ± 6.28	18.94 ± 26.28	18.68 ± 0.96	9.91 ± 0.84	18.85 ± 1.30	26.69 ± 1.21	25.68 ± 1.15
Mean	4.59 ± 1.06	5.35 ± 1.69	3.49 ± 1.12	5.45 ± 2.42	12.02 ± 7.26	$ 17.36 \pm 12.21 $	13.74 ± 6.72	6.93 ± 4.23	15.29 ± 6.60	22.30 ± 7.95	22.42 ± 6.74

Table 3: Calibration error (ECE $\times 100$) for various methods on CIFAR-10, CIFAR-100, and TinyImageNet (mean \pm std over 3 runs; lower is better). Our ATS-CP variants (left block) consistently achieve lower ECE than the baseline calibration methods (right block). Best in bold, second best underlined.

We measure calibration error using the *Conformal Prediction Set Mass Error* (CPSME) at level α :

$$\text{CPSME}_\alpha(p, \hat{p} \mid x_*) = \left| \sum_{y \in C_\alpha^*(x_*)} (p(y \mid x_*) - \hat{p}(y \mid x_*)) \right|,$$

where $\hat{p}(y \mid x_*)$ is the final output of our calibration procedure (that might be aggregated over different levels α).

This metric captures the discrepancy between the true probability mass and the calibrated mass over the ground-truth conformal set. A well-calibrated model achieves CPSME close to zero. Unlike the Expected Calibration Error (formally introduced in the next section), which considers only the maximum predicted probability (typically referred to as “confidence”), CPSME accounts for all significant classes within the conformal set.

Table 2 reports CPSME averaged over $\alpha \in \{0.05, \dots, 0.50\}$ and five random seeds (see Appendix F for details). In this Table, “CondNF” stands for conditional normalizing flow; “MultiQR” stands for multihead quantile regressor. Overall, our methods substantially outperform all baselines in terms of CPSME. In particular, ATS-MAQ (MultiQR) attains the lowest error (0.0777), followed by ATS-GQ (score). As expected, no method achieves perfect calibration on this task, but our adaptive approaches clearly align the predicted probabilities much closer to the true distribution than the alternatives. Next, we evaluate these methods on standard image classification benchmarks.

5.3 Image Classification Datasets

We evaluate our methods on three standard image classification datasets (CIFAR-10, CIFAR-100 [15], TinyImageNet [17]). As a primary metric, our experiments use *Expected Calibration Error (ECE)*. This is a widely used calibration error metric [9]. The idea is to partition the predicted confidences (maximal predicted probabilities) into M bins and compute the weighted average of the absolute difference between bin accuracy and average confidence:

$$\text{ECE} = \sum_{m=1}^M \frac{|B_m|}{n} |\text{Acc}(B_m) - \text{Conf}(B_m)|.$$

A model that is perfectly calibrated will satisfy $\text{Acc}(B_m) = \text{Conf}(B_m)$ in every bin, yielding $\text{ECE} = 0$.

We evaluate different calibration methods on CIFAR-10 (10 classes), CIFAR-100 (100 classes), and TinyImageNet (200 classes). We train a ResNet-18 [10] model on each dataset’s training set and use 10,000 validation samples per dataset. We further split each validation set into three parts: 4,000 for calibrating the model, 4,000 for training any auxiliary calibration models (e.g., quantile regressors), and 2,000 for testing.

Calibration results. Table 3 reports mean \pm std ECE $\times 100$ for each method on the three datasets. As expected, the contaminated base model shows the worst calibration (highest ECE), confirming that our noise injection successfully induced miscalibration. All methods improve ECE to some extent compared to the base model. Notably, our α -specific ATS-CP-GQ and ATS-CP-AQ achieve the lowest ECE on all three datasets. The α -agnostic ATS-CP-MAQ also outperforms most standard methods, making it a practical choice when a specific α is hard to preselect. Even though our techniques focus on coverage rather than ECE optimization, they remain competitive in calibration performance. More details on experiments are provided in Appendix E.

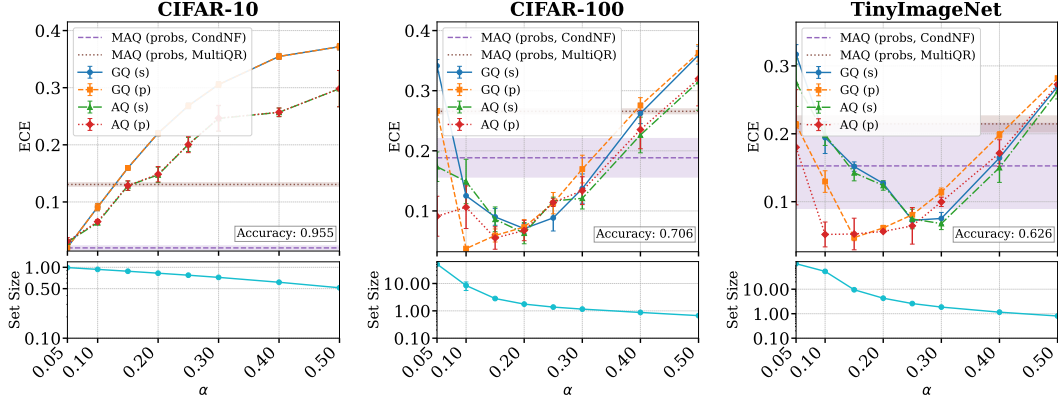


Figure 3: Effect of miscoverage rate α on calibration and set size. The top panels plot ECE versus α for fixed- α ATS-CP variants (solid curves) with shaded regions and error bars indicating \pm one standard deviation; the bottom panels show the average conformal set size for classical CP. Dashed horizontal lines denote α -agnostic ATS-CP-MAQ methods, which require no prespecified miscoverage rate.

5.4 Ablation on the Choice of Miscoverage Rate

Figure 3 illustrates how the ECE of our methods and the average conformal set size vary with the miscoverage rate α on three image classification datasets: CIFAR-10, CIFAR-100, and TinyImageNet. Each dataset exhibits a different optimal α for minimum ECE, showing that selecting an appropriate miscoverage rate is a crucial practical decision. This dataset-dependent sensitivity reflects an inherent feature of conformal prediction rather than a shortcoming of our framework. To avoid manual tuning, we introduced two α -agnostic ATS-CP-MAQ variants—CondNF (conditional normalizing flow) and MultiQR (multihead quantile regressor)—which are shown as horizontal dashed lines. While these α -agnostic methods match the best fixed- α variants on CIFAR-10, their calibration quality degrades on CIFAR-100 and TinyImageNet under the same training-set size, indicating that reliable α -agnostic calibration requires sufficient model capacity or training data. We also observe that when the base classifier is nearly perfect (CIFAR-10, with set size close to one even for small α), increasing α for our methods is less efficient than for less accurate base models.

6 Limitations

Some methods we suggested depend on choosing a miscoverage rate α , and our strongest results come from these approaches. To ease this, we propose adaptive, α -agnostic variants that remove the need for manual selection. These methods often match fixed- α performance but require extra models and can be too sensitive to complex score distributions. We combine multiple calibrated vectors by simple averaging; more advanced aggregation (e.g., weighted averaging) may improve results. This work is a first step toward conformal calibration (including fully α -agnostic approaches), and future work should refine both the α -agnostic methods and the vector-aggregation strategies.

7 Conclusion

We have introduced Adaptive Temperature Scaling with Conformal Prediction (ATS-CP)—the first post-hoc, distribution-free framework that endows conformal prediction sets with instance-wise calibrated probabilities. Our approach is model-agnostic (no retraining), distribution-free, and easily integrates with any pre-trained classifier. We introduced a family of methods of varying complexity: some select a fixed miscoverage rate α and adaptively calibrate the resulting probabilities, while others operate without any pre-specified α . Our experiments on standard image classification benchmarks demonstrate that these approaches provide reliable calibration and effectively match the required coverage levels.

References

- [1] Anastasios N Angelopoulos, Stephen Bates, et al. Conformal prediction: A gentle introduction. *Foundations and Trends® in Machine Learning*, 16(4):494–591, 2023.
- [2] Sergio A Balanya, Juan Maroñas, and Daniel Ramos. Adaptive temperature scaling for robust calibration of deep neural networks. *Neural Computing and Applications*, 36(14):8073–8095, 2024.
- [3] Lev M Bregman. The relaxation method of finding the common point of convex sets and its application to the solution of problems in convex programming. *USSR computational mathematics and mathematical physics*, 7(3):200–217, 1967.
- [4] Nicolò Colombo. Normalizing flows for conformal regression. In *Uncertainty in Artificial Intelligence*, pages 881–893. PMLR, 2024.
- [5] Rina Foygel Barber, Emmanuel J Candes, Aaditya Ramdas, and Ryan J Tibshirani. The limits of distribution-free conditional predictive inference. *Information and Inference: A Journal of the IMA*, 10(2):455–482, 2021.
- [6] Vojtech Franc, Daniel Prusa, and Vaclav Voracek. Optimal strategies for reject option classifiers. *Journal of Machine Learning Research*, 24(11):1–49, 2023.
- [7] Yonatan Geifman and Ran El-Yaniv. Selective classification for deep neural networks. *Advances in neural information processing systems*, 30, 2017.
- [8] Tilmann Gneiting and Adrian E Raftery. Strictly proper scoring rules, prediction, and estimation. *Journal of the American statistical Association*, 102(477):359–378, 2007.
- [9] Chuan Guo, Geoff Pleiss, Yu Sun, and Kilian Q Weinberger. On calibration of modern neural networks. In *International conference on machine learning*, pages 1321–1330. PMLR, 2017.
- [10] Kaiming He, Xiangyu Zhang, Shaoqing Ren, and Jian Sun. Deep residual learning for image recognition. In *Proceedings of the IEEE conference on computer vision and pattern recognition*, pages 770–778, 2016.
- [11] Jianguo Huang, Huajun Xi, Linjun Zhang, Huaxiu Yao, Yue Qiu, and Hongxin Wei. Conformal prediction for deep classifier via label ranking. In *Proceedings of the 41st International Conference on Machine Learning*, pages 20331–20347, 2024.
- [12] Eyke Hüllermeier and Willem Waegeman. Aleatoric and epistemic uncertainty in machine learning: An introduction to concepts and methods. *Machine learning*, 110(3):457–506, 2021.
- [13] Tom Joy, Francesco Pinto, Ser-Nam Lim, Philip HS Torr, and Puneet K Dokania. Sample-dependent adaptive temperature scaling for improved calibration. In *Proceedings of the AAAI Conference on Artificial Intelligence*, volume 37, pages 14919–14926, 2023.
- [14] Sanyam Kapoor, Wesley J Maddox, Pavel Izmailov, and Andrew G Wilson. On uncertainty, tempering, and data augmentation in bayesian classification. *Advances in neural information processing systems*, 35:18211–18225, 2022.
- [15] Alex Krizhevsky, Geoffrey Hinton, et al. Learning multiple layers of features from tiny images. 2009.
- [16] Meelis Kull, Miquel Perello Nieto, Markus Kängsepp, Telmo Silva Filho, Hao Song, and Peter Flach. Beyond temperature scaling: Obtaining well-calibrated multi-class probabilities with dirichlet calibration. *Advances in neural information processing systems*, 32, 2019.
- [17] Yann Le and Xuan Yang. Tiny imagenet visual recognition challenge. *CS 231N*, 7(7):3, 2015.
- [18] Weitang Liu, Xiaoyun Wang, John Owens, and Yixuan Li. Energy-based out-of-distribution detection. *Advances in neural information processing systems*, 33:21464–21475, 2020.
- [19] Rafael Müller, Simon Kornblith, and Geoffrey E Hinton. When does label smoothing help? *Advances in neural information processing systems*, 32, 2019.

- [20] Vincent Plassier, Alexander Fishkov, Victor Dheur, Mohsen Guizani, Souhaib Ben Taieb, Maxim Panov, and Eric Moulines. Rectifying conformity scores for better conditional coverage. *ICML*, 2025.
- [21] Vincent Plassier, Alexander Fishkov, Mohsen Guizani, Maxim Panov, and Eric Moulines. Probabilistic conformal prediction with approximate conditional validity. *ICLR*, 2024.
- [22] John Platt et al. Probabilistic outputs for support vector machines and comparisons to regularized likelihood methods. *Advances in large margin classifiers*, 10(3):61–74, 1999.
- [23] Yaniv Romano, Evan Patterson, and Emmanuel Candes. Conformalized quantile regression. *Advances in neural information processing systems*, 32, 2019.
- [24] Glenn Shafer and Vladimir Vovk. A tutorial on conformal prediction. *Journal of Machine Learning Research*, 9(3), 2008.
- [25] Ingo Steinwart and Andreas Christmann. Estimating conditional quantiles with the help of the pinball loss. *Bernoulli*, 17(1):211–225, 2011.
- [26] Christian Tomani, Daniel Cremers, and Florian Buettnner. Parameterized temperature scaling for boosting the expressive power in post-hoc uncertainty calibration. In *European conference on computer vision*, pages 555–569. Springer, 2022.
- [27] Huajun Xi, Jianguo Huang, Kangdao Liu, Lei Feng, and Hongxin Wei. Does confidence calibration improve conformal prediction? *arXiv preprint arXiv:2402.04344*, 2024.
- [28] Bianca Zadrozny and Charles Elkan. Transforming classifier scores into accurate multiclass probability estimates. In *Proceedings of the eighth ACM SIGKDD international conference on Knowledge discovery and data mining*, pages 694–699, 2002.

A Existence, Uniqueness, and Coverage of ATS-CP

In this section, we formulate and prove a lemma that shows a unique temperature that can be tuned to meet the desired coverage. Additionally, we discuss the resulting coverage guarantees.

Let $D_{cal} = \{(x_i, y_i)\}_{i=1}^n$ be the calibration dataset, and let a test point x be exchangeable with elements of D_{cal} . Denote by q_α the $\lceil(1 - \alpha)(n + 1)\rceil / n$ -quantile of the empirical score distribution.

Then

$$C_\alpha(x) = \{y: V(x, y) \leq q_\alpha\}$$

is the usual split-conformal set at miscoverage level α . Define

$$f(\tau) = \sum_{y \in C_\alpha(x)} \tilde{p}_V(y | x, \tau),$$

where $\tilde{p}_V(\cdot | x, \tau)$ is defined as in equation (1).

Lemma A.1. *Then:*

1. *If $1 - \alpha$ is greater (or equal) than $\frac{|C_\alpha(x)|}{K}$, then there exists a unique $\tau^* \in [\tau_{\min}, \tau_{\max}]$ such that $f(\tau^*) = 1 - \alpha$.*
2. *The set of labels y , which ordered CDF reaches at least $1 - \alpha$, satisfies the marginal coverage*

$$\Pr(y \in C_\alpha(x)) \geq 1 - \alpha.$$

Proof.

1. **Existence and Uniqueness.** Under mild regularity on the logits, $f(\tau)$ is continuous and strictly monotonic in τ . Then, one can choose τ_{\min}, τ_{\max} so that $f(\tau_{\min}) \leq 1 - \alpha \leq f(\tau_{\max})$ (in practice, we choose $\tau_{\min} = 1e-7, \tau_{\max} = 1e6$). By the Intermediate Value Theorem, there is at least one τ^* with $f(\tau^*) = 1 - \alpha$, and strict monotonicity ensures it is unique.
2. **Marginal Coverage.** Under exchangeability, split-conformal methods guarantee

$$\Pr(y \in C_\alpha(x)) \geq 1 - \alpha.$$

By construction,

$$f(\tau) = \sum_{y \in C_\alpha(x)} \tilde{p}_V(y | x, \tau),$$

so the event $\{f(\tau) \geq 1 - \alpha\}$ is exactly the event $\{y \in C_\alpha(x)\}$. Equivalently, the smallest set of labels whose cumulative probability (when ordered in non-increasing order) reaches at least $1 - \alpha$ contains the true label with probability at least $1 - \alpha$.

□

B Single-tau Minimization

In the main part, Section 3.2, we discussed two options for aggregating several calibrated vectors. However, they may undermine our calibration objectives: each \tilde{p}_j was calibrated so that its entries sum to $1 - \alpha_j$, yet neither p_{avg} nor p_{central} is guaranteed to satisfy a particular coverage level or correspond to any specific temperature parameter.

An alternative is restricting aggregation to the family of tempered softmax distributions and seeking a single temperature τ_* that best unifies all \tilde{p}_j .

Therefore, we derive two ways to choose one ‘‘central’’ tempered categorical vector from $\{\tilde{p}_j\}_{j=1}^M$, each is defined by its temperature τ_j . As before, inspired by the method described in Section 3.2, will look at *forward* and *reverse* KL objectives over the family of tempered probabilities.

In both of these cases, we are aiming to find an optimal τ^* for our candidate probability, that is, a tempered softmax of scores: $\tilde{p}_V^{(\tau)} = \text{Softmax}\left[-\frac{1}{\tau} \log V\right]$.

B.1 Forward KL centroid

We choose τ^* to minimize the average *forward* KL from each \tilde{p}_j to our candidate $\tilde{p}_V^{(\tau)}$:

$$\tau^* = \arg \min_{\tau} \frac{1}{M} \sum_{j=1}^M D_{\text{KL}}(\tilde{p}_j \parallel \tilde{p}_V^{(\tau)}),$$

where $D_{\text{KL}}(q \parallel r) = \sum_i q_i \log \frac{q_i}{r_i}$.

B.2 Reverse KL centroid

Alternatively, one can pick τ^* by minimizing the (expected) *reverse* KL :

$$\tau^* = \arg \min_{\tau} \frac{1}{M} \sum_{j=1}^M D_{\text{KL}}(\tilde{p}_V^{(\tau)} \parallel \tilde{p}_j),$$

In both cases, we optimize each objective with respect to τ for 500 iterations. This amount was chosen from a practical (computation feasibility) point of view. Therefore, it may not necessarily lead to convergence.

C General Details on Experiments

We used a CPU and (when neural networks are used) GPU to accelerate computations. Specifically, we run our experiments on Intel i9-10900F (when CPU) and NVIDIA GeForce 2080Ti (when GPU). For one random seed, computations take about 3 hours on the CPU.

D Training Details

In this section, we describe the training details of the proposed methods.

But first, we need a pretrained-based model. We used ResNet-18 models and trained them with cross-entropy loss until loss convergence on the validation split. This results in the models that have the following accuracies: 95.5 for CIFAR-10 (10 classes), 70.56 for CIFAR-100 (100 classes), and 62.61 for TinyImageNet (200 classes).

We can proceed with our proposed procedure using these models and the corresponding validation dataset splits. All three datasets have a validation dataset of size 10,000. We split it into three parts: calibration (4000), training (used for those methods that require it) (4000), and test (2000).

Methods like **ATS-CP-GQ** and **ATS-CP-MGQ** do not require training of auxiliary models. Therefore, they use only calibration split.

In contrast, **ATS-CP-AQ** and **ATS-CP-MAQ** require additional models to perform calibration. Therefore, they use a training dataset for this purpose. An additional option on top of this is to “conformalize” [23] received models, using calibration split as well. Following this idea, we conformalize quantile regression (**ATS-CP-AQ**). All other methods were trained solely on train split; no other data was used.

Now, we describe these auxiliary models in detail.

For **ATS-CP-AQ**, we used a small neural network with two hidden layers with 64 and 16 neurons. As a non-linearity, we used ReLU.

For **ATS-CP-MAQ**, we have two options for auxiliary models. Similarly to **ATS-CP-AQ**, the first is a quantile regression with multiple heads for a preselected set of different α values. In our experiments, we used the following set of specified values of α : [0.05, 0.1, 0.15, 0.2, 0.25, 0.3, 0.4, 0.5]. Therefore, this model has an output of 8, where each component of the output corresponds to the particular quantile of the distribution of scores.

Another option is to use a completely α -agnostic model. We follow the idea of [4], which uses a conditional normalizing flow. This flow has a simple form to ensure the avoidance of quantile crossing. Specifically, we used the one referred to as “Gauss” (see Section 3.2, equation (27) in [4]). We followed the same training process described in the paper and in the accompaniment code.

Method	CIFAR-10	CIFAR-100	TinyImagenet	Mean \pm Std
GQ (prob)	2.02 \pm 0.46	3.74 \pm 0.16	4.72 \pm 0.46	3.49 \pm 1.12
AQ (prob)	3.11 \pm 0.65	5.50 \pm 1.87	5.17 \pm 1.83	4.59 \pm 1.06
AQ (score)	2.98 \pm 0.47	6.30 \pm 1.76	6.77 \pm 0.88	5.35 \pm 1.69
GQ (score)	2.04 \pm 0.46	7.06 \pm 0.82	7.26 \pm 0.89	5.45 \pm 2.41
Isotonic Regression	0.94 \pm 0.36	9.93 \pm 1.11	9.91 \pm 0.84	6.93 \pm 4.23
MAQ (CondNF, avg, probs)	1.96 \pm 0.36	18.84 \pm 3.21	15.27 \pm 6.28	12.02 \pm 7.26
Dirichlet Scaling	4.25 \pm 0.55	18.30 \pm 0.42	18.68 \pm 0.96	13.74 \pm 6.71
MAQ (CondNF, central, probs)	3.42 \pm 0.92	23.22 \pm 3.97	18.84 \pm 7.00	15.16 \pm 8.49
Platt Scaling	6.04 \pm 0.38	20.98 \pm 0.36	18.85 \pm 1.30	15.29 \pm 6.60
ATSC	1.68 \pm 1.03	31.46 \pm 20.67	18.94 \pm 26.28	17.36 \pm 12.21
MAQ (CondNF, avg, scores)	2.00 \pm 0.68	24.32 \pm 1.27	30.45 \pm 3.04	18.92 \pm 12.23
MAQ (MultiQR, central, probs)	13.06 \pm 0.32	26.57 \pm 0.41	21.46 \pm 1.18	20.36 \pm 5.57
MAQ (CondNF, central, scores)	4.21 \pm 0.64	27.10 \pm 1.31	32.49 \pm 2.70	21.27 \pm 12.26
MAQ (MultiQR, avg, scores)	22.29 \pm 0.92	25.13 \pm 1.44	17.84 \pm 0.57	21.75 \pm 3.00
MAQ (MultiQR, avg, probs)	22.29 \pm 0.92	25.40 \pm 1.53	18.32 \pm 0.71	22.00 \pm 2.90
Temperature Scaling	11.16 \pm 0.62	29.07 \pm 0.60	26.69 \pm 1.21	22.30 \pm 7.94
Base Model	13.01 \pm 0.21	28.58 \pm 0.48	25.68 \pm 1.15	22.42 \pm 6.76
MAQ (MultiQR, central, scores)	13.11 \pm 0.28	29.81 \pm 0.70	27.07 \pm 1.61	23.33 \pm 7.31
MGQ (central, scores)	37.16 \pm 0.56	35.93 \pm 1.47	26.95 \pm 0.54	33.34 \pm 4.55
MGQ (avg, scores)	37.16 \pm 0.56	35.93 \pm 1.47	26.95 \pm 0.54	33.34 \pm 4.55
MGQ (central, probs)	37.16 \pm 0.56	36.30 \pm 1.36	28.19 \pm 0.23	33.88 \pm 4.04
MGQ (avg, probs)	37.16 \pm 0.56	36.30 \pm 1.36	28.19 \pm 0.23	33.88 \pm 4.04

Table 4: Extended ECE evaluation on CIFAR-10, CIFAR-100 and TinyImageNet: mean \pm std of the best expected calibration error (ECE \times 100) over three runs for each calibration method. Competitor methods are highlighted in blue; the uncalibrated base model is highlighted in yellow.

E Additional Experimental Results

In this section, we complement the results presented in the main part of the paper. Specifically, we add more instances of our proposed calibration family for completeness. As in the main part of the paper, specifically in Section 5.3, our primary evaluation metric is ECE. To recap, for each of the datasets and different choices of α (for α -specific methods), we computed ECE and reported it. Then, for each α -specific method (dataset-wise), we kept the best α . Similarly to Table 3 from the main part, here we present a similar extended Table 4. Along with the best results we received in terms of ECE, in Table 5, we demonstrate what the best values of α for α -specific methods are.

We see that our α -specific instances (given the optimal choice of α) outperform each competitor over two out of three of the datasets. The closest α -agnostic method, ATS-CP-MAQ on probabilities with CondNF, typically outperforms most competitors and could be a good choice when a good α is unknown.

CIFAR-10 is the only considered dataset where our methods do not beat the baseline. This is linked to the fact that the conformal procedure for this model results in average sets of size equal to or below 1 for the considered set of α values (see bottom of Figure 3). Therefore, our calibration procedure either results in no scaling at all (when the set is empty) or scaling based on only a set of one element, which consists of the most probable class. But this latter situation corresponds to the case when α is small. Therefore, the probability (which is already big) does not change significantly.

F Synthetic Data Experiment Details

In this section, we give a detailed description of our synthetic experiment. The main goal is to create a scenario in which the true label distribution $p(y | x)$ is known exactly. By doing so, we can measure the precise difference between the probabilities estimated by our methods and the ground truth.

We build our ‘‘dataset’’ from a mixture of two-dimensional isotropic Gaussians. There are $K = 10$ components, each centered on a point equally spaced around a circle of radius 2.25. All components

Method	CIFAR-10	CIFAR-100	TinyImagenet
GQ (prob)	0.05	0.1	0.15
AQ (prob)	0.05	0.15	0.1
AQ (score)	0.05	0.2	0.3
GQ (score)	0.05	0.2	0.25

Table 5: Dataset-wise optimal miscoverage rates α for our adaptive quantile (AQ) and global quantile (GQ) calibration methods, chosen to minimize ECE on each dataset.

share the same standard deviation, $\sigma = 0.75$. Thus, we obtain a ten-class classification problem, where each class corresponds to one Gaussian component.

Because we know the density analytically, we can compute the true conditional probabilities at any point x by taking a softmax over the log-densities of each Gaussian:

$$p(y | x) = \text{Softmax}\left(\log \mathcal{N}(x; \mu_y, \sigma^2)\right),$$

where μ_y is the center of the y -th Gaussian and $\mathcal{N}(x; \mu_y, \sigma^2)$ denotes its density.

We use the CPSME_α metric to quantify calibration error rather than the more common ECE. Unlike ECE, CPSME_α looks at the set of the most “significant” classes instead of only the single top-confidence class:

$$\text{CPSME}_\alpha(p, \hat{p} | x_*) = \left| \sum_{y \in C_\alpha^*(x_*)} (p(y | x_*) - \hat{p}(y | x_*)) \right|.$$

Here, $C_\alpha^*(x)$ is the smallest set of labels whose true probabilities sum to at least $1 - \alpha$. Concretely, we sort the values $p(y | x)$ in descending order and include labels until the cumulative sum first exceeds $1 - \alpha$:

$$C_\alpha^*(x) = \{y_{(1)}, y_{(2)}, \dots, y_{(k)}\} \quad \text{such that} \quad \sum_{j=1}^{k-1} p(y_{(j)} | x) < 1 - \alpha \leq \sum_{j=1}^k p(y_{(j)} | x).$$

By comparing the total true probability mass and the total calibrated probability mass over this set $C_\alpha^*(x)$, we directly measure how well our calibration method matches the ground truth on the most important classes.

Table 6 presents the complete set of results. For each $\alpha \in \{0.05, 0.1, 0.15, 0.2, 0.25, 0.3, 0.4, 0.5\}$, we report CPSME_α averaged over five random seeds. The rightmost column shows all eight levels’ average CPSME_α . We sort the methods in ascending order by this final column so that the best-performing methods appear at the top.

To assist the reader, we highlight:

- *Blue*: competing calibration methods
- *Orange*: the base model using raw (contaminated) probabilities
- *Red*: single-tau methods (see Section B)

We omit the “ATS-CP” prefix in our method names for brevity and display only the distinguishing part.

The table shows that our proposed methods — in particular, MAQ with MultiQR, MGQ, GQ, and AQ — outperform all the competitors. It is especially encouraging that the α -agnostic variants consistently rank at the top.

By contrast, the single-tau methods perform poorly in this setting. We suspect this is due to limited optimization: we restrict each method to 500 gradient steps, which may not be sufficient for these objectives to converge fully.

G Verbose Description of Proposed Methods

This section provides a detailed, step-by-step explanation of each ATS-CP variant. Our goal is to give readers a comprehensive view of the ideas and algorithms behind our framework.

Method	0.05	0.1	0.15	0.2	0.25	0.3	0.35	0.4	0.45	0.5	Avg. (over α -s)
MAQ (MultiQR, avg. probs)	0.026 \pm 0.005	0.041 \pm 0.006	0.052 \pm 0.005	0.062 \pm 0.004	0.072 \pm 0.004	0.084 \pm 0.004	0.096 \pm 0.004	0.108 \pm 0.005	0.117 \pm 0.006	0.122 \pm 0.006	0.078 \pm 0.005
MAQ (MultiQR, central, probs)	0.020 \pm 0.003	0.036 \pm 0.003	0.049 \pm 0.002	0.060 \pm 0.002	0.071 \pm 0.003	0.085 \pm 0.004	0.099 \pm 0.005	0.112 \pm 0.007	0.124 \pm 0.009	0.130 \pm 0.009	0.079 \pm 0.005
MAQ (MultiQR, central, scores)	0.034 \pm 0.006	0.035 \pm 0.004	0.041 \pm 0.002	0.051 \pm 0.002	0.064 \pm 0.003	0.081 \pm 0.004	0.102 \pm 0.005	0.124 \pm 0.007	0.146 \pm 0.009	0.163 \pm 0.009	0.084 \pm 0.005
MAQ (MultiQR, avg. scores)	0.045 \pm 0.007	0.043 \pm 0.006	0.047 \pm 0.004	0.055 \pm 0.003	0.067 \pm 0.004	0.082 \pm 0.004	0.100 \pm 0.005	0.119 \pm 0.007	0.137 \pm 0.007	0.151 \pm 0.007	0.085 \pm 0.006
GQ (score, alpha=0.1)	0.078 \pm 0.003	0.068 \pm 0.003	0.064 \pm 0.002	0.064 \pm 0.002	0.069 \pm 0.002	0.078 \pm 0.002	0.090 \pm 0.002	0.104 \pm 0.002	0.119 \pm 0.002	0.129 \pm 0.002	0.086 \pm 0.002
AQ (score, alpha=0.05)	0.041 \pm 0.018	0.047 \pm 0.021	0.055 \pm 0.022	0.064 \pm 0.021	0.076 \pm 0.020	0.091 \pm 0.018	0.109 \pm 0.017	0.128 \pm 0.014	0.146 \pm 0.013	0.157 \pm 0.013	0.092 \pm 0.018
GQ (score, alpha=0.05)	0.050 \pm 0.004	0.047 \pm 0.004	0.051 \pm 0.004	0.059 \pm 0.004	0.071 \pm 0.004	0.087 \pm 0.004	0.107 \pm 0.003	0.128 \pm 0.002	0.150 \pm 0.003	0.167 \pm 0.003	0.092 \pm 0.003
MQQ (avg. scores)	0.044 \pm 0.001	0.050 \pm 0.001	0.057 \pm 0.001	0.065 \pm 0.001	0.076 \pm 0.002	0.098 \pm 0.001	0.108 \pm 0.002	0.127 \pm 0.003	0.145 \pm 0.005	0.158 \pm 0.005	0.092 \pm 0.002
AQ (score, alpha=0.1)	0.070 \pm 0.012	0.066 \pm 0.013	0.066 \pm 0.013	0.070 \pm 0.012	0.078 \pm 0.012	0.089 \pm 0.011	0.103 \pm 0.011	0.118 \pm 0.010	0.133 \pm 0.009	0.143 \pm 0.007	0.094 \pm 0.011
GQ (score, alpha=0.15)	0.105 \pm 0.001	0.097 \pm 0.001	0.088 \pm 0.001	0.084 \pm 0.001	0.083 \pm 0.001	0.085 \pm 0.001	0.091 \pm 0.001	0.099 \pm 0.001	0.105 \pm 0.002	0.109 \pm 0.002	0.095 \pm 0.001
AQ (score, alpha=0.15)	0.094 \pm 0.008	0.088 \pm 0.008	0.084 \pm 0.008	0.082 \pm 0.007	0.085 \pm 0.007	0.091 \pm 0.007	0.100 \pm 0.006	0.118 \pm 0.006	0.123 \pm 0.005	0.098 \pm 0.007	
AQ (prob, alpha=0.25)	0.059 \pm 0.007	0.075 \pm 0.008	0.093 \pm 0.008	0.098 \pm 0.007	0.103 \pm 0.008	0.111 \pm 0.008	0.119 \pm 0.007	0.126 \pm 0.006	0.127 \pm 0.005	0.100 \pm 0.007	
MQQ (central, scores)	0.032 \pm 0.006	0.044 \pm 0.001	0.055 \pm 0.002	0.066 \pm 0.002	0.080 \pm 0.003	0.098 \pm 0.003	0.121 \pm 0.004	0.145 \pm 0.005	0.171 \pm 0.007	0.197 \pm 0.01	0.101 \pm 0.004
AQ (prob, alpha=0.2)	0.062 \pm 0.005	0.075 \pm 0.005	0.093 \pm 0.005	0.099 \pm 0.005	0.105 \pm 0.005	0.113 \pm 0.005	0.124 \pm 0.006	0.137 \pm 0.006	0.159 \pm 0.005	0.165 \pm 0.005	0.105 \pm 0.005
GQ (score, alpha=0.2)	0.115 \pm 0.007	0.111 \pm 0.006	0.105 \pm 0.007	0.115 \pm 0.006	0.126 \pm 0.007	0.136 \pm 0.006	0.143 \pm 0.007	0.152 \pm 0.008	0.162 \pm 0.008	0.174 \pm 0.007	0.116 \pm 0.007
AQ (prob, alpha=0.15)	0.059 \pm 0.002	0.077 \pm 0.002	0.087 \pm 0.003	0.096 \pm 0.002	0.105 \pm 0.002	0.115 \pm 0.002	0.126 \pm 0.002	0.134 \pm 0.002	0.139 \pm 0.002	0.137 \pm 0.002	0.116 \pm 0.002
AQ (prob, alpha=0.15)	0.057 \pm 0.010	0.076 \pm 0.011	0.087 \pm 0.012	0.097 \pm 0.012	0.107 \pm 0.012	0.119 \pm 0.012	0.132 \pm 0.011	0.142 \pm 0.011	0.150 \pm 0.009	0.151 \pm 0.007	0.112 \pm 0.011
AQ (prob, alpha=0.2)	0.074 \pm 0.012	0.092 \pm 0.013	0.101 \pm 0.014	0.110 \pm 0.014	0.116 \pm 0.015	0.120 \pm 0.015	0.124 \pm 0.016	0.128 \pm 0.016	0.131 \pm 0.016	0.130 \pm 0.015	0.113 \pm 0.015
MQQ (central, probs)	0.047 \pm 0.002	0.070 \pm 0.002	0.084 \pm 0.003	0.096 \pm 0.004	0.108 \pm 0.005	0.122 \pm 0.006	0.136 \pm 0.009	0.147 \pm 0.011	0.156 \pm 0.013	0.163 \pm 0.017	0.113 \pm 0.007
AQ (prob, alpha=0.35)	0.073 \pm 0.014	0.093 \pm 0.015	0.103 \pm 0.016	0.112 \pm 0.016	0.120 \pm 0.016	0.126 \pm 0.016	0.129 \pm 0.016	0.130 \pm 0.016	0.131 \pm 0.015	0.128 \pm 0.014	0.114 \pm 0.015
GQ (prob, alpha=0.2)	0.074 \pm 0.002	0.092 \pm 0.002	0.102 \pm 0.001	0.109 \pm 0.002	0.115 \pm 0.002	0.124 \pm 0.002	0.132 \pm 0.001	0.140 \pm 0.002	0.143 \pm 0.002	0.139 \pm 0.002	0.117 \pm 0.002
GQ (score, alpha=0.2)	0.141 \pm 0.001	0.135 \pm 0.001	0.127 \pm 0.001	0.119 \pm 0.001	0.113 \pm 0.001	0.109 \pm 0.002	0.107 \pm 0.002	0.108 \pm 0.003	0.108 \pm 0.004	0.104 \pm 0.003	0.117 \pm 0.002
AQ (score, alpha=0.25)	0.140 \pm 0.008	0.136 \pm 0.008	0.130 \pm 0.008	0.124 \pm 0.007	0.124 \pm 0.007	0.128 \pm 0.006	0.136 \pm 0.006	0.140 \pm 0.006	0.146 \pm 0.005	0.150 \pm 0.006	0.118 \pm 0.006
AQ (prob, alpha=0.1)	0.062 \pm 0.021	0.083 \pm 0.024	0.096 \pm 0.026	0.108 \pm 0.026	0.120 \pm 0.026	0.134 \pm 0.026	0.147 \pm 0.026	0.157 \pm 0.025	0.164 \pm 0.023	0.165 \pm 0.022	0.124 \pm 0.024
GQ (prob, alpha=0.1)	0.066 \pm 0.006	0.089 \pm 0.007	0.101 \pm 0.008	0.113 \pm 0.008	0.124 \pm 0.008	0.136 \pm 0.008	0.146 \pm 0.005	0.154 \pm 0.005	0.156 \pm 0.007	0.156 \pm 0.006	0.124 \pm 0.007
AQ (prob, alpha=0.05)	0.061 \pm 0.032	0.083 \pm 0.036	0.098 \pm 0.036	0.110 \pm 0.036	0.122 \pm 0.036	0.136 \pm 0.035	0.148 \pm 0.035	0.158 \pm 0.033	0.164 \pm 0.031	0.165 \pm 0.029	0.125 \pm 0.034
AQ (prob, alpha=0.4)	0.079 \pm 0.011	0.101 \pm 0.012	0.112 \pm 0.013	0.122 \pm 0.013	0.132 \pm 0.014	0.141 \pm 0.014	0.146 \pm 0.016	0.148 \pm 0.016	0.146 \pm 0.016	0.143 \pm 0.015	0.127 \pm 0.014
GQ (prob, alpha=0.25)	0.091 \pm 0.002	0.109 \pm 0.002	0.118 \pm 0.002	0.126 \pm 0.002	0.130 \pm 0.002	0.140 \pm 0.002	0.145 \pm 0.002	0.146 \pm 0.002	0.140 \pm 0.002	0.140 \pm 0.002	0.128 \pm 0.002
Isotonic Regression	0.067 \pm 0.008	0.087 \pm 0.009	0.101 \pm 0.011	0.113 \pm 0.011	0.126 \pm 0.012	0.142 \pm 0.014	0.157 \pm 0.016	0.169 \pm 0.017	0.177 \pm 0.018	0.180 \pm 0.020	0.132 \pm 0.014
MQQ (avg. probs)	0.083 \pm 0.004	0.103 \pm 0.004	0.115 \pm 0.003	0.124 \pm 0.003	0.133 \pm 0.003	0.143 \pm 0.003	0.152 \pm 0.003	0.159 \pm 0.003	0.162 \pm 0.005	0.160 \pm 0.007	0.133 \pm 0.004
GQ (prob, alpha=0.3)	0.104 \pm 0.002	0.123 \pm 0.003	0.132 \pm 0.003	0.140 \pm 0.003	0.146 \pm 0.003	0.149 \pm 0.003	0.151 \pm 0.003	0.151 \pm 0.003	0.151 \pm 0.002	0.143 \pm 0.002	0.139 \pm 0.003
GQ (score, alpha=0.25)	0.176 \pm 0.001	0.172 \pm 0.001	0.165 \pm 0.001	0.157 \pm 0.001	0.146 \pm 0.001	0.135 \pm 0.001	0.128 \pm 0.001	0.126 \pm 0.002	0.116 \pm 0.003	0.103 \pm 0.003	0.142 \pm 0.002
AQ (score, alpha=0.3)	0.177 \pm 0.010	0.176 \pm 0.009	0.170 \pm 0.009	0.164 \pm 0.009	0.155 \pm 0.010	0.141 \pm 0.011	0.129 \pm 0.012	0.124 \pm 0.013	0.117 \pm 0.013	0.112 \pm 0.013	0.146 \pm 0.011
AQ (prob, alpha=0.45)	0.093 \pm 0.011	0.119 \pm 0.012	0.133 \pm 0.012	0.144 \pm 0.012	0.155 \pm 0.013	0.165 \pm 0.012	0.172 \pm 0.012	0.175 \pm 0.012	0.174 \pm 0.011	0.168 \pm 0.010	0.150 \pm 0.012
GQ (prob, alpha=0.35)	0.116 \pm 0.002	0.137 \pm 0.002	0.148 \pm 0.002	0.156 \pm 0.002	0.164 \pm 0.002	0.169 \pm 0.002	0.170 \pm 0.002	0.169 \pm 0.002	0.165 \pm 0.002	0.154 \pm 0.001	0.155 \pm 0.002
GQ (prob, alpha=0.05)	0.097 \pm 0.011	0.123 \pm 0.011	0.138 \pm 0.012	0.149 \pm 0.011	0.160 \pm 0.012	0.170 \pm 0.011	0.179 \pm 0.010	0.187 \pm 0.009	0.180 \pm 0.009	0.175 \pm 0.008	0.155 \pm 0.010
Platt Scaling	0.094 \pm 0.009	0.122 \pm 0.011	0.138 \pm 0.011	0.150 \pm 0.011	0.163 \pm 0.011	0.175 \pm 0.011	0.186 \pm 0.012	0.194 \pm 0.013	0.197 \pm 0.016	0.194 \pm 0.017	0.161 \pm 0.012
Base Model	0.099 \pm 0.001	0.125 \pm 0.001	0.141 \pm 0.001	0.153 \pm 0.002	0.164 \pm 0.003	0.177 \pm 0.002	0.188 \pm 0.002	0.196 \pm 0.003	0.200 \pm 0.003	0.198 \pm 0.003	0.164 \pm 0.002
AQ (score, alpha=0.35)	0.203 \pm 0.011	0.203 \pm 0.013	0.198 \pm 0.014	0.192 \pm 0.015	0.184 \pm 0.014	0.170 \pm 0.015	0.152 \pm 0.015	0.136 \pm 0.016	0.126 \pm 0.015	0.118 \pm 0.013	0.168 \pm 0.014
Temperature Scaling	0.106 \pm 0.001	0.133 \pm 0.001	0.148 \pm 0.001	0.160 \pm 0.001	0.171 \pm 0.001	0.183 \pm 0.001	0.193 \pm 0.001	0.201 \pm 0.002	0.203 \pm 0.003	0.200 \pm 0.002	0.170 \pm 0.001
GQ (score, alpha=0.3)	0.209 \pm 0.001	0.209 \pm 0.002	0.203 \pm 0.002	0.195 \pm 0.002	0.184 \pm 0.002	0.168 \pm 0.002	0.				

Main idea. For the ground truth distribution over labels $p(y | x)$ and its ideal conformal set $C_\alpha^*(x)$, we have

$$\sum_{y \in C_\alpha^*(x)} p(y | x), \geq 1 - \alpha,$$

where

$$C_\alpha^*(x) = \{y_{(1)}, y_{(2)}, \dots, y_{(k)}\} \quad \text{such that} \quad \sum_{j=1}^{k-1} p(y_{(j)} | x) < 1 - \alpha \leq \sum_{j=1}^k p(y_{(j)} | x).$$

We mimic this behavior by introducing a family of *tempered* probabilities $\tilde{p}(y | x, \tau)$ and selecting an input-specific temperature τ_α so that for the chosen conformal set

$$\sum_{y \in C_\alpha(x)} \tilde{p}(y | x, \tau_\alpha) \geq 1 - \alpha.$$

We find $\tau_\alpha > 0$ satisfying this via a simple binary search.

The probability is defined as follows. Given any nonnegative score $V(x, y)$, define

$$\tilde{p}(y | x, \tau) = \text{Softmax}\left(-\frac{1}{\tau} \log V(x, y)\right),$$

so that as $\tau \rightarrow 0$ the mass concentrates on the smallest-score labels, and as $\tau \rightarrow \infty$ it spreads uniformly.

Calibration Methods

Let the calibration dataset be

$$D_{\text{cal}} = \{(x_i, y_i)\}_{i=1}^n \longrightarrow D_{\text{cal}}^V = \{(x_i, V_i)\}_{i=1}^n, \quad V_i = V(x_i, y_i).$$

We describe two families of methods.

α -specific methods

These variants require fixing a global miscoverage rate α by a user in advance for all inputs, like in a standard conformal prediction setup.

Inspired by two branches of conformal predictions, namely **marginal CP** and **conditional CP**, we suggest two methods under this family. The first method, **ATS-CP-GQ** (Global Quantile), follows standard (marginal) CP approach – quantile of scores distribution q_α is selected on the D_{cal}^V only once, and it remains constant for all the inputs x . Therefore, the resulting sets are not adaptive and might not be tight. This is a known problem of marginal CP, which is as severe as more heterogeneous label noise across covariates.

To address this, people adapt **conditional CP**. There are multiple ways to reach (approximate) conditional coverage. But all of them more-less boil down to predicting an adaptive quantile $q_\alpha(x)$ for each covariate. One possible and straightforward approach to make it is to train a model (e.g., Quantile Regression - QR) that will predict a $q_\alpha(x)$ quantile of the distribution of the scores for a given input x . This model can be trained using a pinball loss [25] and optionally “conformalized” on top of this [23]. Therefore, for each input x , the QR model provides a more accurate estimation of the quantile $q_\alpha(x)$. Once it is calculated, we proceed as usual – build a conformal set $C_\alpha(x)$ and tune τ_α to satisfy the cumulative mass condition. We call this method **ATS-CP-AQ** (Adaptive Quantile).

In short, to summarize:

1. Global Quantile (ATS-CP-GQ).

Compute the $(1 - \alpha)$ -quantile q_α of the calibration scores D_{cal}^V , that is fixed and used for all input objects x . For each test input x , define

$$C_\alpha(x) = \{y: V(x, y) \leq q_\alpha\},$$

then find $\tau^*(x)$ via binary search so that $\sum_{y \in C_\alpha(x)} \tilde{p}(y | x, \tau^*) = 1 - \alpha$.

2. Adaptive Quantile (ATS-CP-AQ).

Train a quantile regressor QR_α on $\{(x_i, V_i)\}$ to predict the input-dependent threshold $q_\alpha(x)$. At test time:

$$C_\alpha(x) = \{y: V(x, y) \leq \text{QR}_\alpha(x)\},$$

and again solve for τ^* satisfying the coverage constraint.

α -agnostic methods

As emphasized many times in the main part of the paper, setting a miscoverage rate α is important for the CP procedure in general and, in particular, for the suggested CP-based probability calibration. Therefore, a general desideratum is to have an α -agnostic approach. Even though an α -agnostic method may not always match the performance of the optimal α -specific method, it can still be a compelling and safe choice – especially when the optimal α is unknown. That alone is already a meaningful advantage if it consistently performs better than a range of reasonable (but potentially suboptimal) fixed α values.

Similarly to the approaches in α -specific approaches, we can do two conceptual things here. Say our calibration dataset $D_{cal}^V = \{(x_i, V_i)\}_{i=1}^n$ consists of n pairs x_i, V_i of covariates and scores. This induces an empirical distribution of scores. Each element of this empirical distribution corresponds to a particular α , and there are n such α -values. If one makes this correspondence between score V_i and the corresponding α_i , this results into the dataset: $D_{cal}^V = \{(x_i, V_i)\}_{i=1}^n \rightarrow D_{cal}^\alpha = \{(V_i, \alpha_i)\}_{i=1}^n$.

In other words, one corresponds each element of the calibration dataset of scores to a particular level of α (so that each element of this dataset is potential quantile with corresponding miscoverage rate α).

Next, at *online* stage of our proposed algorithm, for a new input x , we compute all possible scores (as usual in conformal prediction) for each possible label y . Therefore, in the case of the classification over K classes, we have K possible scores for each input x . Next, we correspond each of these scores with D_{cal}^α , and retrieve K corresponding quantiles (basically for each of K scores we find the minimal element among D_{cal}^α , that exceeds it) and collect the corresponding α_k . Next, we calibrate probabilities that correspond to each set, for each of these extracted α_k , which results in $\{\tilde{p}_\theta(y \mid x, \tau_{\alpha_k})\}_{k=1}^K$. Next, we need to aggregate these vectors somehow. So the feature of this method is that it is α -agnostic, fully operates with the calibration dataset and does not require training of any additional models. In this sense, it is close to the ATS-CP-GQ methods. We call this methodology **ATS-CP-MGQ** (multiple global quantiles). However, if we want our conformal sets to be adaptive for the covariates, one needs to do something similar to ATS-CP-AQ.

Here is where our **ATS-CP-MAQ** comes into play. What one can do is to specify a set of α values in advance (without betting everything on a single α) and train, for example, a Multihead quantile regression. It is similar to APS-CP-AQ – one specifies several α values and fits a model to predict the multiple quantiles of the distributions of the scores. And then one proceeds as in ATS-CP-MGQ – we have $\{\tilde{p}_\theta(y \mid x, \tau_{\alpha_k})\}_{k=1}^{|\alpha|}$ (where $|\alpha|$ is the number of α -values one selected to train MultiQR) and need to aggregate them somehow.

Another approach is to train a model (conditional normalizing flow [4]) that will transform the conditional distribution of scores to a simple distribution (e.g., Standard Gaussian), for which we know quantiles analytically (or at least it is simple to calculate). Then, for a new input x , we compute K possible scores (one for each label), and using this conditional normalizing flow, we map each of these scores to the simple distribution. Knowing the image, we can calculate CDF, and, as 1 - CDF, we can calculate α_k . Next, we proceed in the same way as before – for each α_k we have $\{\tilde{p}_\theta(y \mid x, \tau_{\alpha_k})\}_{k=1}^K$ and need to aggregate them somehow.

To summarize:

3. Multi-Global Quantiles (ATS-CP-MGQ).

Given input x , for each class y , estimate its empirical miscoverage $\alpha_y = 1 - \hat{F}_V(V(x, y))$ on the calibration set. For each distinct α_y , form the set $C_{\alpha_y}(x)$ and calibrate a temperature τ_y . This yields multiple calibrated distributions $\{\tilde{p}(y \mid x, \tau_y)\}$. We aggregate these by a centroid (see below).

4. Multi-Adaptive Quantiles (ATS-CP-MAQ).

Fit a conditional normalizing flow to map each score $V(x, y)$ to a simple reference distribution (e.g., $\mathcal{N}(0, 1)$). For a new x , transform each score to an effective miscoverage α_y via the learned CDF, predict the corresponding quantile $q_{\alpha_y}(x)$, and calibrate τ_y as above. This method adapts both the set threshold and temperature per instance.

Aggregation of Calibrated Distributions

After obtaining multiple calibrated vectors $\{\tilde{p}_j\}_{j=1}^m$ (e.g. one per α_j), we aggregate them into a single categorical distribution via a Bregman centroid under the Kullback–Leibler divergence:

$$p_{\text{avg}} = \arg \min_p \sum_{j=1}^m D_{\text{KL}}(\tilde{p}_j \parallel p) = \frac{1}{m} \sum_{j=1}^m \tilde{p}_j,$$

$$p_{\text{central}} = \arg \min_p \sum_{j=1}^m D_{\text{KL}}(p \parallel \tilde{p}_j) = \text{Softmax}\left(\frac{1}{m} \sum_{j=1}^m \log \tilde{p}_j\right).$$